RFX3 governs growth and beating efficiency of motile cilia in mouse and controls the expression of genes involved in human ciliopathies

Loubna El Zein[1], Aouatef Ait-Lounis[2], Laurette Morlé[1], Joëlle Thomas[1], Brigitte Chhin[1], Nathalie Spassky[3], Walter Reith[2] and Bénédicte Durand[1,*]

[1]Université de Lyon, Lyon, F-69003, Université Lyon 1, CNRS, UMR5534, CGMC, Centre de Génétique Moléculaire et Cellulaire, Villeurbanne, F-69622, France
[2]Department of Pathology and Immunology, Faculty of Medicine, University of Geneva, CMU, 1 rue Michel-Servet, CH-1211 Geneva, Switzerland
[3]INSERM U711, Hôpital Salpêtrière, 47 Boulevard de l'hôpital, 75013 Paris, France
*Author for correspondence (durand-b@univ-lyon1.fr)

Accepted 21 June 2009
Journal of Cell Science 122, 3180-3189 Published by The Company of Biologists 2009
doi:10.1242/jcs.048348

Summary

Cilia are cellular organelles that play essential physiological and developmental functions in various organisms. They can be classified into two categories, primary cilia and motile cilia, on the basis of their axonemal architecture. Regulatory factor X (RFX) transcription factors have been shown to be involved in the assembly of primary cilia in *Caenorhabditis elegans*, *Drosophila* and mice. Here, we have taken advantage of a novel primary-cell culture system derived from mouse brain to show that RFX3 is also necessary for biogenesis of motile cilia. We found that the growth and beating efficiencies of motile cilia are impaired in multiciliated *Rfx3*$^{-/-}$ cells. RFX3 was required for optimal expression of the FOXJ1 transcription factor, a key player in the differentiation program of motile cilia. Furthermore, we demonstrate for the first time that RFX3 regulates the expression of axonemal dyneins involved in ciliary motility by binding directly to the promoters of their genes. In conclusion, RFX proteins not only regulate genes involved in ciliary assembly, but also genes that are involved in ciliary motility and that are associated with ciliopathies such as primary ciliary dyskinesia in humans.

Supplementary material available online at
http://jcs.biologists.org/cgi/content/full/122/17/3180/DC1

Key words: Axonemal dyneins, Cilia, Mouse primary cell cultures, Primary ciliary dyskinesia, RFX proteins

Introduction

Cilia play key roles in various organisms ranging from cell or fluid motility to cellular responses to environmental cues (for reviews, see Eggenschwiler and Anderson, 2007; Singla and Reiter, 2006). In the last decade, numerous studies have highlighted the importance of cilia in human health and the consequences of ciliary dysfunction in several human diseases (for reviews, see Bisgrove and Yost, 2006; Fliegauf et al., 2007; Marshall, 2008). Tremendous effort has also been devoted to the identification of proteins involved in cilia assembly (Andersen et al., 2003; Avidor-Reiss et al., 2004; Broadhead et al., 2006; Keller et al., 2005; Li et al., 2004; Ostrowski et al., 2002; Pazour et al., 2005; Stolc et al., 2005), leading to the establishment of gene lists compiled in freely available databases [cilia proteome or ciliome data bases (Gherman et al., 2006; Inglis et al., 2006)]. Recent work has added probable new candidates to these primary lists (Hayes et al., 2007; Lonergan et al., 2006; McClintock et al., 2008; Ross et al., 2007; Stubbs et al., 2008; Yu et al., 2008). These studies used complementary approaches based on proteomic and transcriptomic methods as well as comparative genomic strategies. Several studies took advantage of the specificity of the regulatory factor X (RFX) family of transcription factors for a well-defined DNA motif: the X-box (Emery et al., 1996b). This approach was pioneered by studies in *Caenorhabditis elegans* and was subsequently extended to other comparative studies and models.

RFX transcription factors have been shown to govern ciliogenesis in *C. elegans* and *Drosophila*, and this property has been instrumental in both organisms for identifying novel genes involved in ciliogenesis (Avidor-Reiss et al., 2004; Blacque et al., 2005; Chen et al., 2006; Dubruille et al., 2002; Efimenko et al., 2006; Efimenko et al., 2005; Haycraft et al., 2003; Haycraft et al., 2001; Li et al., 2004; Schafer et al., 2003; Swoboda et al., 2000). In mice, RFX3 has been shown to regulate primary ciliary growth in the embryonic node and in the pancreas (Ait-Lounis et al., 2007; Bonnafe et al., 2004). In both systems, RFX3 was found to regulate at least one gene coding for a molecular motor component of the intraflagellar transport (IFT) apparatus: the dynein light chain gene *Dync2li1*. In addition, RFX3 deficiency leads to hydrocephalus that is associated with defects in the differentiation of the subcommissural organ and choroid plexuses (Baas et al., 2006).

We show here that RFX3 is a key player in the formation of motile multicilia in a primary-cell culture system derived from mouse brain. RFX3 deficiency affects both ciliary growth and ciliary beat frequency (CBF) in this culture system. In addition to the previously known *Dync2li1*, RFX3 was found to regulate the orthologs of genes involved in primary ciliary dyskinesia (PCD) in humans. We show that RFX3 binds to the promoters of the genes encoding two axonemal dyneins involved in ciliary motility. We also demonstrate that RFX3 regulates *Foxj1* expression by binding to its promoter. Our results thus show that mammalian RFX proteins regulate genes involved in ciliary assembly per se but also control genes involved in ciliary motility. In addition, our work validates a novel cell culture system for functional studies on genes implicated in ciliogenesis in mice.

Results

In vitro differentiation of ciliated ependymal cells derived from E18.5 mouse embryos

During mouse embryogenesis, *Rfx3* is strongly expressed in a subset of cerebral ventricular cells (Baas et al., 2006). After birth, the expression of *Rfx3* is maintained in multiciliated ependymal cells lining the cerebral ventricles (Fig. 1A). This timing and pattern of expression is in agreement with the fact that *Rfx3* is expressed in the multiciliated ependymal cell lineage from progenitors to the fully mature stage (Spassky et al., 2005). When backcrossed onto a pure C57BL/6 genetic background, no $Rfx3^{-/-}$ pups survived more than a few days after birth. It was hence very difficult to assess ciliary motility or growth in vivo in these mice, because ciliogenesis of ependymal cells is only completed after birth in mice (Spassky et al., 2005). To evaluate the function of *Rfx3* in ependymal ciliogenesis, we took advantage of a neural-stem-cell culture system established from mouse embryos (Fig. 1B). In this system, embryonic day (E)18.5 embryonic mouse brains are dissected, the lateral ventricular zones are dissociated and cells are plated on a laminin substrate. Upon confluence, neural stem cells are separated from neurons or oligodendrocytes on the basis of cell adhesive properties by vigorous overnight shaking of the cultures and are then replated at a defined density (see Materials and Methods). The selected cells express the neuronal-stem-cell marker nestin (supplementary material Fig. S1A) and the astrocyte cell marker GFAP (supplementary material Fig. S1B). A single primary cilium is observed on the majority of cells (70%) at confluence (Fig. 1C, arrows). The cell cultures are highly homogenous after the selection procedure. Only low residual numbers of oligodendrocytes or neuronal cells remain after this selection procedure (generally less than 1%, but always less than 5%). Serum starvation induces the stem cells to differentiate into a monolayer of ciliated cells as demonstrated by staining for the tight-junction marker ZO1 and the cilia marker anti-glu-α-tubulin (supplementary material Fig. S1D). These cells express CD24, a cell surface marker of ependymocytes (Calaora et al., 1996) (supplementary material Fig. S1E). Cells progressively develop motile cilia. After 20 days of serum starvation, numerous motile cilia are visible on the majority of cells (Fig. 1C; supplementary material Fig. S1C and Movie 1). No changes are observed in cell number during differentiation, as estimated by counting nuclei before and after differentiation. The only cells that die during the first 4 days of serum deprivation are the few (<1%) contaminating neuronal or oligodendritic cells that are easily distinguished and not included in the cell count at day 0.

Rfx3 is expressed in ependymal cell culture

RFX3 expression was visualized by immunostaining of the cell cultures. Nuclear RFX3 was evident at day 0 before serum starvation in 95-99% of the cells (Fig. 1C; Fig. 2A, around 1% of the cells never express RFX3). We observed a reproducible increase in RFX3 expression during serum starvation. Because anti-RFX3 antibodies do not allow the detection of RFX3 on western blots, RFX3 protein was quantified by confocal microscopy. A significant increase in RFX3 immunoreactivity was observed after 20 days of serum deprivation (Fig. 2B). To determine whether the in-vitro-induced ciliogenesis is accompanied by an increase in cilia-specific gene expression, we performed a kinetic analysis of the expression of a series of representative ciliary genes (Fig. 2C). Statistical significance of the variations at each stage relative to day 0 was evaluated by two-tailed paired Student's *t*-test. We observed a small (2.5-fold) but significant increase in *Rfx3* messenger levels ($P<0.05$ for day 8 to 20). We also observed that the expression of mRNA for genes known to be necessary for cilia assembly, such as *Dync2li1* or *Bbs4*, were increased at least 1.5-fold. Known motility genes such as *Dnahc5*, *Dnahc9* and *Dnahc11* were induced more than threefold after serum starvation. Expression of the transcription-factor-encoding *Foxj1* gene was strongly increased during the first days of serum starvation but diminished after 8 days of differentiation. Maximal induction for all

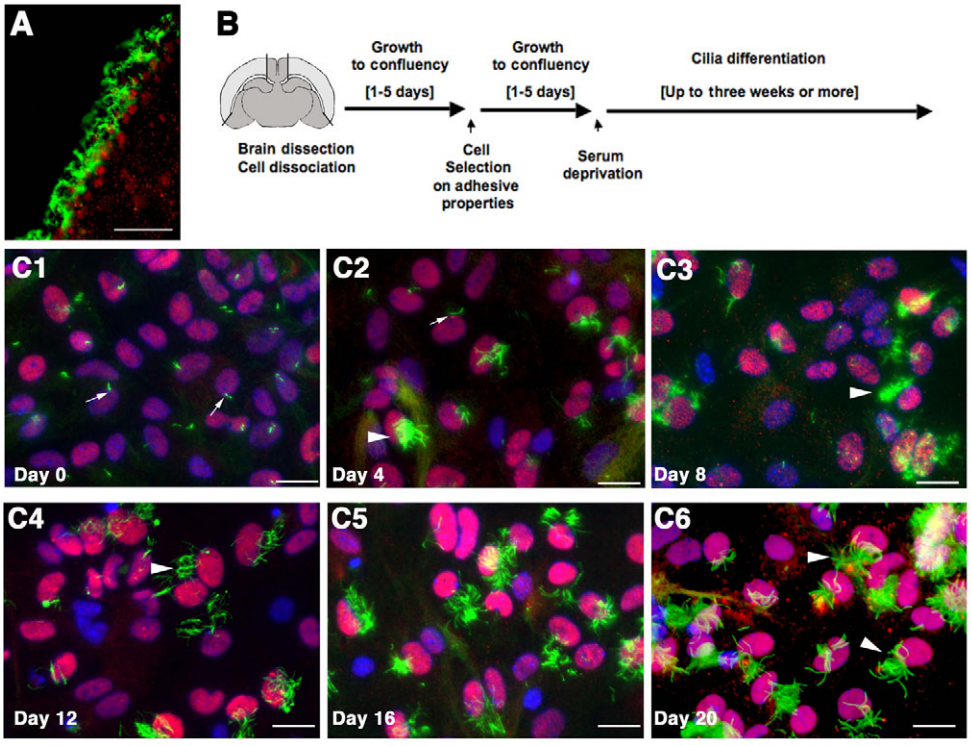

Fig. 1. RFX3 is expressed in ciliated ependymal cells in vivo and during ependymal ciliogenesis in vitro. (A) RFX3 is expressed in ciliated ependymal cells lining the ventricles in postnatal mouse brains. The image shows the lateral ventricle of an adult mouse brain stained for RFX3 (red) and βIV tubulin (green). Scale bar: 50 µm. (B) Schematic representation of the cell culture protocol. E18.5 embryonic brains were dissected, the cortical lateral hemispheres (light grey) were dissociated and cells were cultured as indicated. (C) Representative images of ependymal cell cultures before (C1, day 0) and after (C2-C6: days 4, 8, 12, 16 or 20, respectively) serum deprivation. RFX3 (red), cilia (green) and nuclei (blue) were visualized by immunostaining. Note that cells first harbor a primary cilium (C1, arrows) and progressively develop multiple cilia (C2-C6, arrowheads). At 20 days after serum deprivation, most cells carry a tuft of cilia (C6). Approximately 1% of the cells never express RFX3. Scale bars: 20 µm.

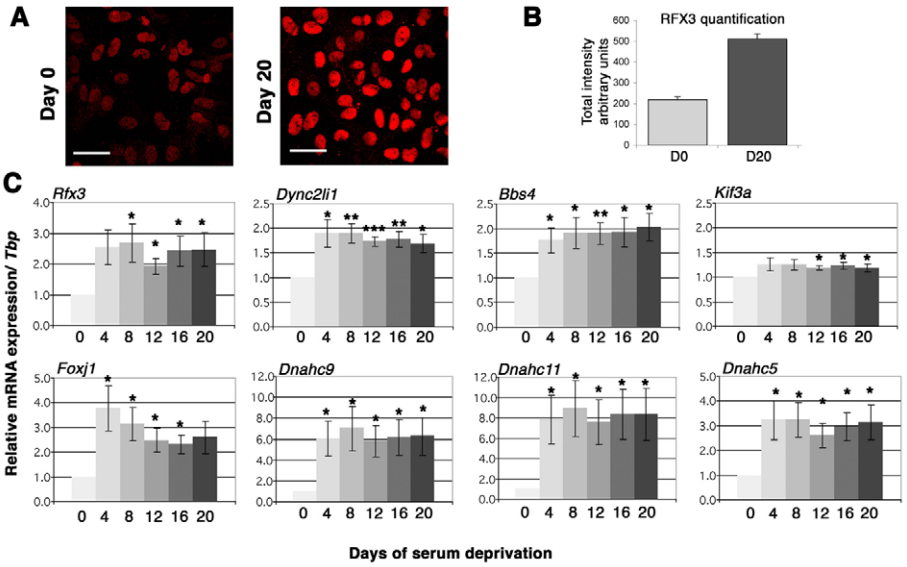

Fig. 2. Ciliary gene expression is increased during in vitro ciliogenesis. (A) RFX3 protein expression before (day 0) and after (day 20) differentiation was visualized on 3D projections of confocal stacks acquired with identical settings (raw 3D images, no signal adjustment). Scale bars: 50 µm. (B) Quantification of RFX3 protein levels at day 0 (D0) and day 20 (D20) by confocal imaging and quantification by MetaMorph analysis. (C) Time course of ciliary gene expression following serum deprivation. mRNA abundance was quantified by real-time RT-PCR on five or six independent cultures. The expression level of each gene was normalized to the housekeeping gene *Tbp* (TATA binding protein). The results were expressed relative to the values at day 0 (set at 1). The expression of most ciliogenic genes increases during serum deprivation (*Rfx3*, *Dync2li1*, *Dnahc5*, *Dnahc9*, *Dnahc11*, *Foxj1*). Two-tailed paired Student's *t*-test analysis was performed to evaluate significant variations relative to day 0. **P*<0.05, ***P*<0.01, ****P*<0.001.

of the other analyzed ciliogenic genes was observed after 8 days of serum starvation. This timing precedes the maximum density of cilia and ciliated cells in the culture (Fig. 1C; supplementary material Fig. S1C). *Kif3a* gene expression was induced weakly, whereas expression of the control cell-proliferation marker gene *Mki67* was reduced during serum starvation (not shown).

Rfx3-deficient ependymal cells show a strong reduction in ciliary growth

To assess the function of *Rfx3* in ciliogenesis, we compared parallel cell cultures obtained from wild-type and *Rfx3*$^{-/-}$ littermates. We determined by immunolabeling that no nuclear RFX3 protein was detected in *Rfx3*$^{-/-}$-derived cells (Fig. 3A). We did not observe any

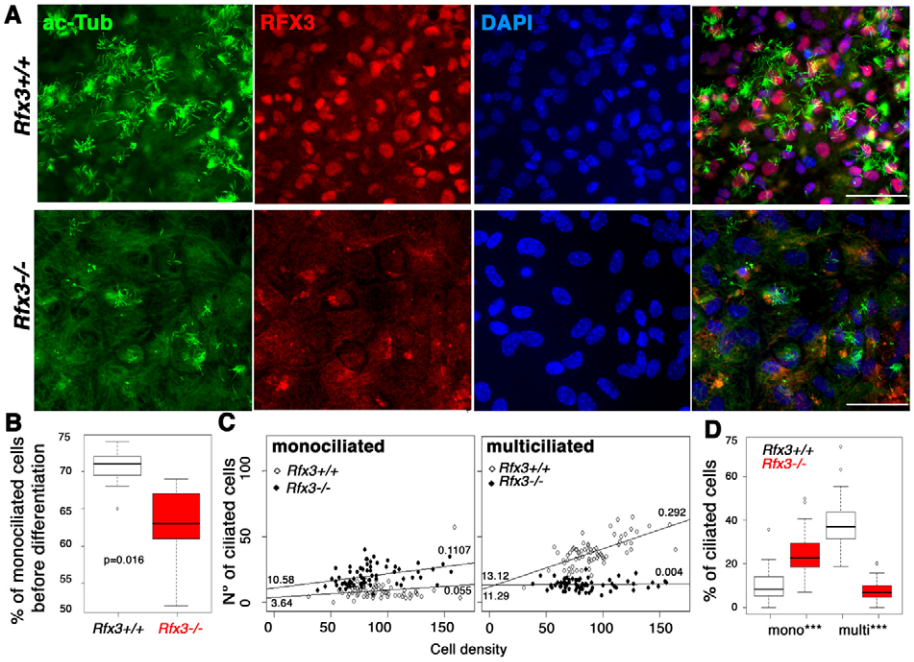

Fig. 3. The number of cilia/cell is reduced in *Rfx3*$^{-/-}$ ependymal cell cultures. (A) Images of cells after 16 days of serum deprivation from representative cultures derived from wild-type (upper row) or *Rfx3*$^{-/-}$ (lower row) embryos, stained with anti-acetylated α-tubulin (green), anti-RFX3 (red) and DAPI (blue). Merged images are shown on the right. Scale bars: 50 µm. (B) Distribution of the average number of monociliated cells before serum deprivation in *Rfx3*$^{-/-}$ (red) and *Rfx3*$^{+/+}$ (white) samples. The number of monociliated cells is slightly but significantly (ANOVA analysis, *P*=0.016) reduced in *Rfx3*$^{-/-}$ samples. (C) Ciliated cells at day 16 were counted in a blinded manner for a total of 14 different samples (seven *Rfx3*$^{+/+}$ and seven *Rfx3*$^{-/-}$) from six different littermates. For each sample, ten different fields were photographed and cells were classified on the basis of their number of cilia and counted. The number of ciliated cells was reported as a function of cell density to demonstrate that the difference in multiciliated cell numbers between wild-type and *Rfx3*$^{-/-}$ samples is not biased by a difference in cell density. The values of the slopes and intercepts are presented, respectively, on the right and on the left of each regression line. Differences in linear regression slopes are statistically significant between the two genotypes for multiciliated cells ($P=3.03\times10^{-10}$), but not monociliated cells (*P*=0.24). (D) Distribution of the average fractions (expressed in % of total cell number) of mono- and multiciliated cells for *Rfx3*$^{-/-}$ (red) and *Rfx3*$^{+/+}$ (white) samples at day 16. ***The differences between *Rfx3*$^{-/-}$ and wild-type samples are statistically significant for mono- and multiciliated cells (ANOVA analysis, $P<2.2\times10^{-16}$).

difference in expression of the precursor-specific marker GFAP or nestin before differentiation (supplementary material Fig. S1A,B), suggesting that RFX3 has no major effects on the overall cell-selection procedure. We observed a small difference in the number of primary cilia before differentiation in *Rfx3*$^{-/-}$ samples compared with wild type (Fig. 3B). This is in agreement with our previously published observation that RFX3 controls primary-ciliary growth, even though the effect is less pronounced in this cell culture system compared with the previously described in vivo situations (Ait-Lounis et al., 2007; Bonnafe et al., 2004).

After serum starvation, we observed drastic differences in the number of multiciliated cells between wild-type and *Rfx3*$^{-/-}$ samples (Fig. 3A,C,D). We quantified the total number of ciliated cells harboring either one cilium or multiple cilia in each sample after 2 weeks of serum starvation (Fig. 3C). To verify that there was no bias resulting from cell-density variations in the cultures due to heterogeneous seeding, we plotted the results as a function of the cell density for each photographed field and the linear regression was calculated. This cell density can vary considerably between fields within one cell culture, even though seeding density was controlled for each experiment. As observed on Fig. 3C, cell density impacted equally on the number of monociliated cells for the two genotypes, because no significant differences could be observed between linear regression slopes (P=0.24). Nevertheless, a larger fraction of the cells remained monociliated after serum deprivation in *Rfx3*$^{-/-}$ samples (Fig. 3D). By contrast, we observed that cell density had a strong impact on the growth of multiple cilia in *Rfx3*$^{+/+}$ cells, whereas multiple ciliary growth was not dependant on cell density in *Rfx3*$^{-/-}$ samples (Fig. 3C, $P=3.03\times10^{-10}$). In addition, the total number of multiciliated cells in *Rfx3*$^{-/-}$ samples was reduced compared with wild type, independently of cell density (Fig. 3D). Thus, *Rfx3* is necessary for ciliogenesis in ependymal cells and controls both the overall frequency of ciliated cells and the number of cilia per cell. After differentiation, we did not observe any difference between the two genotypes in the expression of the ependymal-specific marker CD24 or the cell-junction marker ZO1 (supplementary material Fig. S1D,E), suggesting that defective ciliogenesis does not result from impaired cell-cell contact formation or cell differentiation.

We noticed that cilia were markedly shorter in *Rfx3*$^{-/-}$ cell cultures. We therefore estimated the mean ciliary length of motile cilia on multiciliated cells using confocal microscopy. Three-dimensional (3D) reconstructions were used to visualize the cilia and verify the accuracy of the length measurements. As shown in Fig. 4, ciliary length was significantly reduced in *Rfx3*$^{-/-}$ cells compared with wild type. The mean ciliary length for *Rfx3*$^{-/-}$ cells is 5.5±1.9 µm, which was 57% shorter than for *Rfx3*$^{+/+}$ samples (12.9±1.8 µm). Statistical significance was evaluated using a two-sample Student's *t*-test. The difference in ciliary length was statistically significant ($P<2.2\times10^{-16}$). Thus, *Rfx3* is required for the growth of motile cilia in ependymal cells.

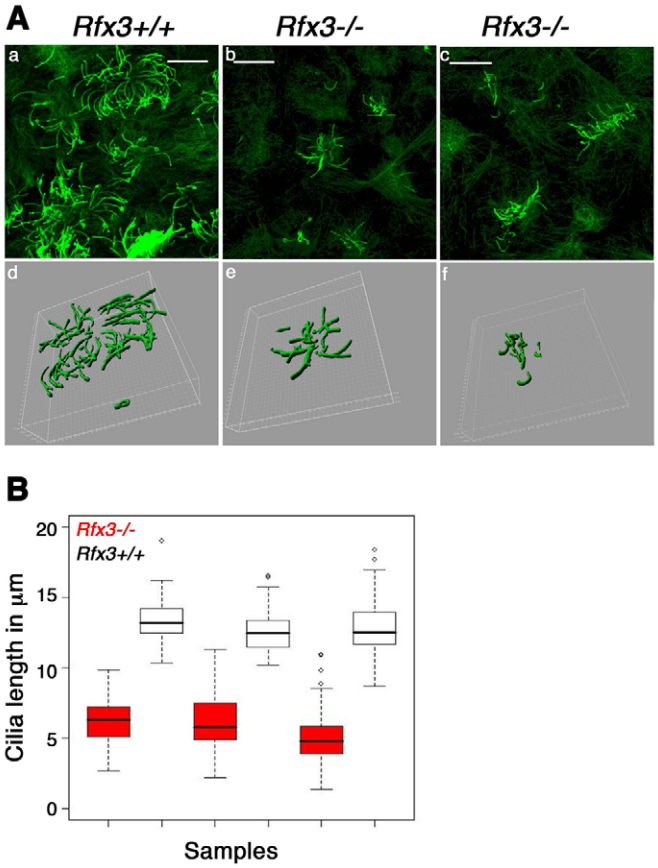

Fig. 4. Cilia are shorter in *Rfx3*$^{-/-}$ ependymal cells. (A) Confocal imaging of cilia stained with anti-acetylated α-tubulin from one representative wild-type (a) and two independent *Rfx3*$^{-/-}$ (b,c) cell cultures at 16 days after serum deprivation. In addition to a reduction in ciliary density, cilia are shorter in *Rfx3*$^{-/-}$ ependymal cells. Scale bar: 15 µm. (d-f) 3D reconstructions of a group of cilia from the upper panels, illustrating the difference in the length of cilia between the two genotypes. Grid scale: 1 µm. (B) The box plot shows the mean cilia length for three *Rfx3*$^{-/-}$ and three *Rfx3*$^{+/+}$ ependymal cell cultures measured in confocal-microscopy stacks. A total of 450 cilia were measured (at least ten cilia/field). Statistical significance of the difference in cilia length was evaluated using a two-sample Student's *t*-test ($P<2.2\times10^{-16}$).

Rfx3-deficient ependymal cells show a reduction of ciliary motility

By videomicroscopy recordings using a high-speed camera, we assessed ciliary motility in cell cultures derived from wild-type and *Rfx3*$^{-/-}$ embryos. Striking differences were observed in slow-speed videos of the cells (see representative examples in supplementary material Movies 2 and 3). We precisely quantified the mean CBF for each cell. Cells were selected randomly in the cultures and the measurement was performed for six to nine fields for each culture (for each field the measurement was performed for one to three cells). To check that the calculated CBF differences were not affected by environmental factors, we measured CBF on samples issued from two different litters (n=seven wild-type samples and n=four *Rfx3*$^{-/-}$ samples) on three different days, at either room temperature or 37°C, and in a random sample order for each day and condition (Fig. 5A). The CBF differences between wild-type and *Rfx3*$^{-/-}$ samples were evident in all of the different situations, even though the absolute CBF value varied between conditions (Fig. 5A). We next repeated the measurements for cultures derived from four additional sets of littermates (Fig. 5B). For each litter, the CBF was significantly reduced in *Rfx3*$^{-/-}$ cells (total number of samples: 17 wild type and 11 *Rfx3*$^{-/-}$). The overall mean CBF for *Rfx3*$^{-/-}$ cilia was 13.3 Hz, and the overall mean CBF for *Rfx3*$^{+/+}$ (wild-type) cilia was 20.14 Hz for all samples. The CBF difference between *Rfx3*$^{-/-}$ and *Rfx3*$^{+/+}$ was statistically significant for all the samples (P<0.05). Thus, *Rfx3* deficiency alters the motility of cilia on in-vitro-differentiated

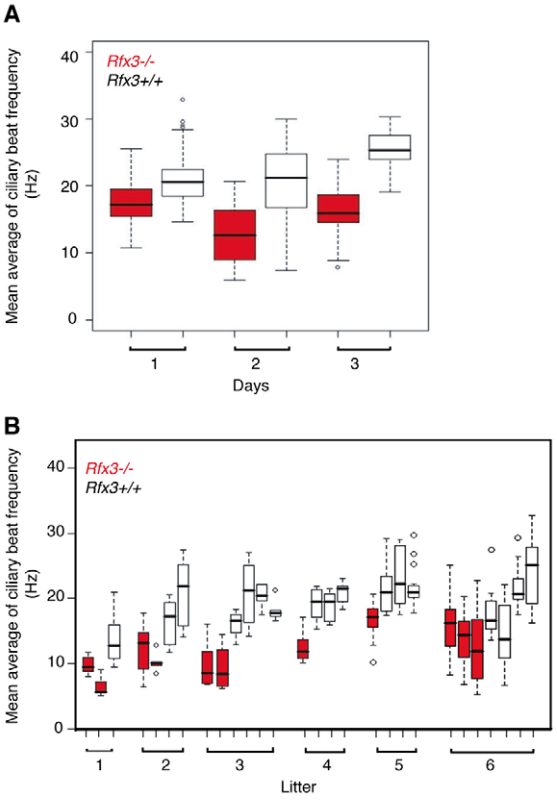

Fig. 5. *Rfx3*$^{-/-}$ ependymal cells have a reduced CBF. (A) CBF measurements were made for mutant (n=4) and wild-type (n=7) samples from litters 5 and 6 on three separate days and at room temperature (days 1-2) or 37°C (day 3). ANOVA analysis shows that the CBF difference between *Rfx3*$^{-/-}$ and *Rfx3*$^{+/+}$ samples is statistically significant (P=6×10^{-4}). (B) CBF for *Rfx3*$^{-/-}$ (red) and wild-type (white) cultures from six independent litters. Statistical analysis using a linear mixed effect model demonstrates that the difference in CBF between *Rfx3*$^{-/-}$ and *Rfx3*$^{+/+}$ cultures is statistically significant in each experiment (P<0.05). ANOVA analysis also shows that CBF values are dependant on the *Rfx3* genotype for all samples (P<0.0001).

primary ependymal cells. We also observed that cilia beating was more frequently asynchronous in *Rfx3*$^{-/-}$ cells compared with wild-type cells (compare supplementary material Movies 2 and 3), although a few cells showing asynchronous beating were generally observed even in wild-type samples (data not shown).

Finally, we compared by transmission electron microscopy the ultrastructure of cilia between *Rfx3*$^{-/-}$ and wild-type cultures. We did not observe defects in the basal-body ultrastructure in *Rfx3*$^{-/-}$ samples (supplementary material Fig. S2). Whereas numerous cilia were visualized in transverse sections in wild-type samples, only a few transverse sections of cilia could be observed in the mutant samples. Hence, it was difficult to visualize stereotyped ultrastructural defects in the mutant cilia and no clear mechanistic conclusions could be drawn from this ultrastructural analysis. Cilia with normal architecture were visualized in the mutant samples but cilia with perturbed microtubule arrangements were frequently observed. These defects seemed to affect mainly the distal region of the cilia (supplementary material Fig. S2), suggesting improper axonemal elongation in the mutant cilia. It should be noted that aberrant cilia were also occasionally observed in wild-type samples.

Ciliary genes are downregulated in *Rfx3*-deficient ependymal cells

RFX proteins regulate a similar set of genes involved in ciliogenesis in *C. elegans* and *Drosophila*. Several RFX target genes identified in these two organisms are involved in IFT (Avidor-Reiss et al., 2004; Blacque et al., 2005; Chen et al., 2006; Efimenko et al., 2006; Efimenko et al., 2005; Haycraft et al., 2003; Haycraft et al., 2001; Laurencon et al., 2007; Li et al., 2004; Schafer et al., 2003; Swoboda et al., 2000). In addition, the expression of *Drosophila* and nematode orthologs of genes involved in the Bardet-Biedl syndrome (BBS) is also regulated by RFX proteins (Ansley et al., 2003; Blacque et al., 2005; Chen et al., 2006; Efimenko et al., 2005; Laurencon et al., 2007). We therefore investigated whether RFX3 also regulates the expression of these conserved ciliary genes in mice. We analyzed a selection of IFT and BBS genes (Fig. 6). The expression of *Dync2li1* was significantly downregulated in *Rfx3*$^{-/-}$ samples. *Bbs4* expression was slightly reduced in the mutant samples compared with wild type in each litter, but this difference was not statistically significant (P=0.125) when all wild-type and mutant samples were compared together. By contrast, *Bbs2* expression was not affected in *Rfx3*$^{-/-}$ samples. The control *Rps9* gene encoding ribosomal protein 9 showed no significant difference in expression between wild-type and *Rfx3*$^{-/-}$ samples.

Drosophila genes involved in ciliary motility have been found to share an X-box in two *Drosophila* species (Laurencon et al., 2007). Among these motility genes, two axonemal dynein genes, *CG9492* and *CG3723*, are under *Rfx* control in *Drosophila* (Laurencon et al., 2007) (our unpublished results). Their orthologues in mammals are *Dnahc5* and *Dnahc9*, respectively. We analyzed the expression of these genes in our cell culture system, together with *Dnahc11*, a paralog of *Dnahc9* that is also homologous to *CG3723*. The expression of *Dnahc5*, *Dnahc11* and *Dnahc9* was strongly downregulated in *Rfx3*$^{-/-}$ cell cultures, and these genes are thus under *Rfx3* control in mice (Fig. 6). Because *Dnahc11* and *Dnahc9* are under the control of *Foxj1* (Brody et al., 2000; Chen et al., 1998; Stubbs et al., 2008; Yu et al., 2008), we investigated whether *Rfx3* might also regulate the *Foxj1* gene. We observed a modest but significant reduction in *Foxj1* expression (P=0.0428) in *Rfx3*$^{-/-}$ samples (Fig. 6). We can therefore not exclude that downregulation of *Dnahc11* and *Dnahc9* expression in *Rfx3*$^{-/-}$ samples could be an indirect consequence of the minor reduction in *Foxj1* expression.

Ciliary genes are direct targets of RFX3 in ciliated ependymal cells

To determine whether RFX3 directly regulates ciliary gene expression, we performed chromatin immunoprecipitation (ChIP) experiments. Crosslinked chromatin from large-scale cultures of ependymal cells from wild-type newborn pups was immunoprecipitated with anti-RFX3 antibodies. Immunoprecipitates were then amplified by quantitative PCR using primers situated upstream of the expected transcription start sites of six of the candidate RFX3 target genes identified by our expression analysis (see above). Primers situated at randomly selected downstream positions within the genes were used as negative controls. Our results demonstrated that the promoters of *Bbs4*, *Dync2li1*, *Dnahc11* and *Dnahc9* are selectively enriched in the RFX3 ChIP samples and are thus bound by RFX3 in the cultured ependymal cells (Fig. 7A). Analysis of the promoter sequences of these genes in several mammalian genomes revealed the presence of highly conserved X-boxes situated immediately upstream of the

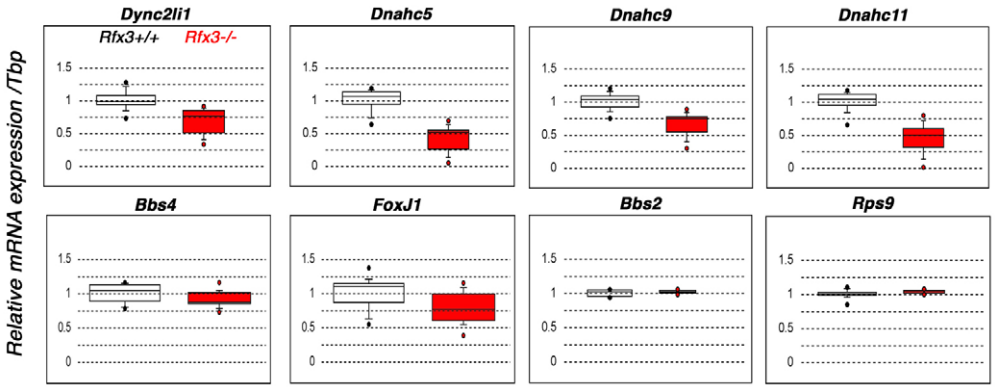

Fig. 6. Ciliary gene expression is downregulated in *Rfx3*$^{-/-}$ samples. Box-plot representation of mRNA abundance. Real-time RT-PCR was performed on RNA extracted from wild-type (n=10) and *Rfx3*$^{-/-}$ (n=5) samples from three independent litters. Kruskal-Wallis non-parametric analysis of variance was performed and is significant for *Dync2li1* (P=0.0101), *Dnahc11* (P=0.0033), *Dnahc5* (P=0.0033), *Dnahc9* (P=0.0071) and *Foxj1* (P=0.0428). For *Bbs4* (P=0.1275), the variations are not statistically significant. No variations are observed for *Bbs2* and *Rps9*. For *Foxj1* and *Bbs4*, n=14 wild-type and n=11 *Rfx3*$^{-/-}$ samples were quantified. Results were normalized using *Tbp*.

transcription start sites of the *Dnahc9*, *Dync2li1* and *Bbs4* genes (Fig. 7B). No conserved X-box was evident in the promoter proximal region of the *Dnahc11* gene. However, a strongly conserved X-box was observed immediately downstream (+80 nucleotides) of the transcription start site in several mammalian genomes. Enrichment of the *Dnahc11* promoter in our ChIP experiments could be the consequence of RFX3 binding to this downstream site. No binding of RFX3 to the *Dnahc5* promoter was detected despite the fact that it contains an X-box-like sequence situated upstream of the transcription start site. Alignment of the X-box motifs found in the promoters analyzed in this study reveals that the *Dnahc5* X-box contains changes at highly conserved nucleotides of the X-box consensus site, suggesting that these residues are crucial for the binding of RFX3 (Fig. 7C). *Dnahc5* is thus either regulated indirectly by RFX3 or controlled by an X-box motif that remains to be localized but would have to be situated outside of the 2-kb upstream region that was analyzed by ChIP. *Foxj1* harbors a strongly conserved X-box in its proximal promoter and the *Foxj1* promoter is strongly enriched in the RFX3 ChIP. Together with the small but significant reduction in *Foxj1* expression observed in *Rfx3*$^{-/-}$ cells, these results suggest that binding of RFX3 is required for optimal *Foxj1* expression.

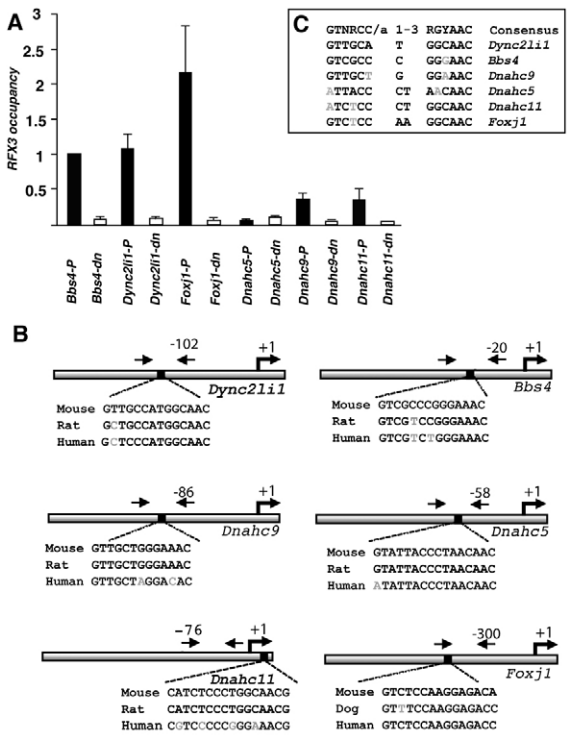

Fig. 7. RFX3 binds to ciliary gene promoters in vivo. (A) Binding of RFX3 to the promoters (-P) of the *Bbs4*, *Dync2li1*, *Dnahc5*, *Dnahc9*, *Dnahc11* and *Foxj1* genes was assessed by quantitative ChIP in OF1 cells. Downstream regions (-dn) were used as negative controls. Results are expressed relative to binding of RFX3 at the *Bbs4* gene in OF1 cells, and show the mean and s.e.m. of three independent experiments. The *Bbs4*, *Foxj1*, *Dync2li1*, *Dnahc9* and *Dnahc11* promoters are occupied by RFX3 in vivo. The *Dnahc5* promoter is not bound by RFX3. (B) RFX3-binding sites (X-boxes) found in the promoters of genes regulated by RFX3 (*Bbs4*, *Dync2li1*, *Dnahc9*, *Foxj1*, *Dnahc11*, *Dnahc5*). Arrows represent the position of the primers used for the quantitative ChIPs presented in A. (C) Alignement of the X-box motifs found in RFX3 target genes compared with the consensus RFX-binding motif (Emery et al., 1996b). Note that promoters occupied by RFX3 show an X-box motif that is conserved at the most stringent positions of the GGYAAC half site.

Discussion

The results presented here demonstrate that RFX3 regulates the number, growth and motility of cilia on cultured mouse ependymal cells. We identified genes encoding three axonemal dyneins as novel RFX3-regulated genes. RFX3 binds to the promoters of two of these axonemal dynein genes in vivo. RFX3 therefore regulates two types of genes implicated in cilia biology: genes involved in ciliary assembly (*Dync2li1*, *Foxj1* and *Bbs4*) and genes involved in ciliary motility (*Dnahc11*, *Dnahc9* and *Dnahc5*). This work sets the stage for the identification of target genes of ciliogenic transcription factors in multiciliated mammalian cells.

Transcriptional control of ciliogenesis

A large set of RFX-regulated genes have been defined in *Drosophila* and *C. elegans*. Many of these genes are involved in IFT (Avidor-Reiss et al., 2004; Blacque et al., 2005; Chen et al., 2006; Efimenko et al., 2006; Efimenko et al., 2005; Haycraft et al., 2003; Haycraft et al., 2001; Laurencon et al., 2007; Li et al., 2004; Schafer et al., 2003; Swoboda et al., 2000). These studies have shown that all known

orthologs of Bbs genes are tightly regulated by RFX factors in *Drosophila* and *C. elegans*. We show here that expression of the *Bbs4* gene is not strongly dependant on RFX3 in cultured ependymal cells, despite the fact that RFX3 does bind to the *Bbs4* promoter in vivo. One possible explanation is that other RFX factors might compensate for the absence of RFX3. Although there is only one RFX transcription factor in *C. elegans*, and only two in *Drosophila*, there are seven RFX transcription factors in mammals (Aftab et al., 2008; Emery et al., 1996a). *Rfx2* has been shown to regulate ciliogenesis in the zebrafish (Liu et al., 2007). A role of RFX1 and RFX4-RFX7 in ciliogenesis has so far not been demonstrated. It is possible that functional redundancy between RFX factors is responsible for the mitigated role of RFX3 in *Bbs4* expression. The absence of an effect on *Bbs2* expression in *Rfx3*$^{-/-}$ cells could also reflect a redundancy between RFX factors. Alternatively, it is possible that the requirement for specific RFX factors varies according to the target gene. In this respect, it is not known whether RFX proteins can distinguish between different sets of target genes. RFX1, RFX2 and RFX3 bind to DNA as homo- or heterodimers, and all three bind to the same X-box motifs (Reith et al., 1994). There is currently no experimental evidence suggesting that there are differences in binding affinity or specificity between different RFX dimers.

Rfx genes are expressed differentially in mammalian tissues. For example, *Rfx3* is expressed more strongly in the brain whereas *Rfx2* is expressed strongly in the kidney (Reith et al., 1994). *Rfx4* also exhibits a specific expression pattern (Blackshear et al., 2003; Zhang et al., 2007). The differential expression patterns of RFX transcription factors might help to fine tune ciliogenesis in different cell types. We have shown here that RFX3 is required for the generation of motile cilia in ependymal cells. We have not been able to establish whether RFX3 is also involved in the growth and motility of cilia in the upper airways of the mouse, because *Rfx3*-deficient mice die at birth and ciliogenesis is completed only postnatally in mice (Toskala et al., 2005). However, RFX3 is expressed strongly in ciliated cells of the upper airways towards the end of embryogenesis and throughout postnatal life (our unpublished observations), suggesting that RFX3 could also play a role in ciliogenesis in airways in vivo. We cannot, however, exclude that other RFX transcription factors are also implicated in ciliogenesis of motile cilia in the upper airways.

In addition to genes required for ciliary assembly, we show here that RFX3 regulates several genes encoding axonemal dyneins. A search for X-box motifs led to the identification of several axonemal dynein genes having conserved X-boxes in two *Drosophila* species (Laurencon et al., 2007). We show here that the expression of the *Dnahc9*, *Dnahc11* and *Dnahc5* genes is downregulated in *Rfx3*-deficient ependymal cells. *Dnahc11* and *Dnahc5* are involved in cilia motility in mice and humans (Bartoloni et al., 2002; Ibanez-Tallon et al., 2002; Olbrich et al., 2002; Schwabe et al., 2008; Supp et al., 1997). *Dnahc9* encodes a dynein that is associated with human motile respiratory cilia and exhibits a perturbed distribution in certain patients with PCD (Carson et al., 2002; Fliegauf et al., 2005).

FOXJ1 has been shown to be implicated in ciliogenesis of motile cilia in vertebrates. *Foxj1* expression increases dramatically during in vitro ciliogenesis in multiciliated cells (Ross et al., 2007; You et al., 2004), and *Foxj1*-deficient mice are characterized by the absence of motile cilia (Blatt et al., 1999; Brody et al., 2000; Chen et al., 1998; Tichelaar et al., 1999; Whitsett and Tichelaar, 1999). *Foxj1* has been shown to be sufficient for driving motile cilia assembly in *Xenopus* and zebrafish (Stubbs et al., 2008; Yu et al., 2008). Although *Foxj1* is not sufficient to drive ectopic ciliary growth in mouse epithelial cells (You et al., 2004) and only a few mouse target genes of this transcription factor have been reported (Brody et al., 2000; Chen et al., 1998; Gomperts et al., 2004; Huang et al., 2003), more than 100 target genes have been identified in *Xenopus* (Stubbs et al., 2008; Yu et al., 2008). *Dnahc11* expression depends on *Foxj1* in mice (Brody et al., 2000; Chen et al., 1998) and *Dnahc9* expression depends on *Foxj1* in both *Xenopus* and zebrafish. Interestingly, *Dnahc9* was confirmed to be a direct *Foxj1* target in these animals, and we have shown that *Dnahc9* and *Dnahc11* are direct targets of RFX3 in mice. These observations suggest that RFX and FOXJ1 proteins regulate a common set of ciliary motility genes. RFX3 and FOXJ1 might cooperate to regulate *Dnahc9* and *Dnahc11* expression. In addition, we observed a small but significant reduction in *Foxj1* expression (P=0.0428) in *Rfx3*-deficient cultures, which could amplify the consequences of the loss of *Rfx3* function on *Dnahc9* and *Dnahc11* expression in our cell-culture system.

The HNF1β transcription factor has been shown to be important for ciliogenesis in mouse kidneys (Gresh et al., 2004). ChIP experiments performed with whole kidney tissue led to the identification of HNF1β-binding sites in several ciliogenic genes (Gresh et al., 2004) involved in ciliary assembly or function. However, there is no evidence for a function of HNF1β in multiciliated cells. Recently, the *Noto* transcription factor has been shown to regulate ciliogenesis in mice, and seems to function upstream of both *Rfx3* and *Foxj1* in the embryonic node (Beckers et al., 2007). It would be of particular interest to determine whether *Noto* is involved in the development of multicilia and identify its direct target genes.

We have shown here that our ependymal cell-culture system is suitable for large-scale ChIP experiments, permitting the identification of direct target genes of ciliogenic transcription factors. Multicilia only start to differentiate in the mouse brain and lung epithelia as of E18.5 (Spassky et al., 2005; Toskala et al., 2005). Our cell-culture system allows the isolation of large numbers of ciliated cells from E18.5 embryos and thus permits the analysis of the function of late-embryonic-lethal genes in multiciliated-cell differentiation.

RFX3-binding-site definition

The consensus RFX3-binding site was derived from experiments performed with human RFX1. The consensus RFX1-binding site was defined by in vivo site-selection experiments in yeast (Emery et al., 1996b; Gajiwala et al., 2000). On the basis of this study, X-box-motif searches in *C. elegans* and *Drosophila*, combined with functional studies, led to the identification of consensus X-box motifs in these two organisms. The function of the X-box motif was assayed directly by mutagenesis for several genes in *C. elegans.* In *C. elegans*, the consensus RFX-binding site was precisely defined with a two-nucleotide spacer between the two half sites. In this organism, X-boxes are generally situated within the first 250 nucleotides upstream of the transcription start site. Such a strict position requirement does not seem to be conserved in *Drosophila* (Laurencon et al., 2007) or in mammals. The potential X-box site in *Dnahc11* resides downstream of the transcription start site. Large-scale ChIP experiments have suggested that transcription-factor-binding sites at this position could be underscored in the literature and might be more important than previously anticipated (Koudritsky and Domany, 2008; Tabach et al., 2007). We can, however, not exclude that the true RFX3-binding site in the *Dnahc11* promoter is not the X-box motif found downstream of the transcription start site, but another highly

divergent RFX-binding motif. An alternative possibility is that RFX3 is recruited by interaction with another transcription factor that determines promoter specificity, such as FOXJ1. Combining motif searches with large-scale ChIP data could be very informative for defining the regulatory networks that control ciliogenesis in multiciliated mammalian cells.

RFX proteins and human syndromes

Our results demonstrate that RFX transcription factors regulate two categories of genes: those involved in ciliary assembly and in ciliary motility. The distinction between these two categories was first emphasized by human syndromes resulting from ciliary dysfunction, which can also be classified into two categories corresponding to defects in either ciliary motility or growth. Prototypical examples are PCD and BBS, respectively. These two types of syndrome have been considered to be clinically distinct. However, recent results have revealed previously unnoticed overlaps between these syndromes. For example, recent reports have highlighted the function of BBS proteins in airway respiratory cilia (Shah et al., 2008). Studies in human patients with polycystic kidney diseases have noted a high incidence of bronchiectasis, a previously uncharacterized manifestation of this disease (Driscoll et al., 2008). In addition, some patients with PCD also have retinitis pigmentosa or kidney failure (Bonneau et al., 1993; Moore et al., 2006; Osman et al., 1991). These results suggest that genes involved in BBS might act as modifiers of PCD. Conversely, genes known to be required for ciliary motility could modify the severity of BBS symptoms. In this respect, altered RFX3 function could be responsible for variations in the severity of clinical symptoms in both types of ciliopathy.

Materials and Methods

Mouse strains

Rfx3-deficient mice were generated as previously described (Bonnafe et al., 2004). Wild-type OF1 mouse embryos were used for kinetic studies of ciliogenesis and ChIP experiments. For studies on RFX3 function, experiments were performed with embryos derived from crosses between heterozygous *Rfx3*$^{+/-}$ adults on a C57BL/6 genetic background (Bonnafe et al., 2004). The embryonic stage was estimated on the basis of gestational time, with day 0.5 being defined as the morning when a vaginal plug was detected. Adult mice and embryos were genotyped by PCR as described previously (Bonnafe et al., 2004). Animal experimentation was carried out in a certified animal-housing facility according to procedures approved by the local animal care and experimentation authorities (Ministère Délégué Recherche et Nouvelles Technologies, agreement no. 4936; Direction des Services Vétérinaires, agreement no. 69266 0602).

Ependymal cell culture

All reagents for cell culture were purchased from Gibco Life Technologies. Lateral walls of lateral ventricles were dissected from 18.5 days post-coitum embryos in Hank's medium (HBBS 1× without Ca^{2+} and Mg^{2+}, 0.075% sodium bicarbonate, 0.01 M HEPES and 100 U/ml penicillin-100 µg/ml streptomycin). Cells were trypsinized for 10 minutes at 37°C with 0.01× trypsin followed by centrifugation for 5 minutes at 900 ***g***. Cells were suspended mechanically in DMEM containing 100 U/ml penicillin-100 µg/ml streptomycin and 1.25 µg/ml amphotericin B, and supplemented with 10 % fetal calf serum (FCS). Dissociated cells from a single brain were seeded in two laminin-coated (10 µg/ml) wells of a 24-multiwell plate and maintained in DMEM-10% FCS in a humidified 5% CO_2 atmosphere at 37°C.

At confluence, culture trays were sealed and shaken overnight at 300 rpm (Janke and Kunkel, HS250). Adherent cells were rinsed with PBS and trypsinized. Cells were harvested in DMEM-10 % FCS and seeded on laminin-coated wells as above (two wells/single brain), or polylysine and laminin-coated coverslips (10 µg/ml each) for immunohistochemical analysis. The minimum seeding density at this step was 5×10^4 cells/well in a 24-well culture tray. We used 10^5 seeding density/well in all the experiments presented here. After 24 hours (for 10^5 cells/well seeding density) to 5 days (for lower seeding density), the medium was changed to DMEM without serum to induce cell differentiation. For the culture of ependymal cells from OF1 mice, the brains of ten newborn littermates were pooled and cultured in two flasks of 25 cm^2. After shaking, the cells of each flask were distributed in 24-well tissue-culture trays or in a 100-mm diameter Petri dish coated with laminin and treated as above.

Immunohistochemical analysis

The adherent ependymal cells were fixed in 4% paraformaldehyde for 20 minutes at 4°C, blocked for 1 hour in 5% goat serum, 0.1% Triton X-100 in PBS at room temperature and incubated overnight at 4°C with one of the following antibodies: anti-RFX3 antibody (1/100) (Reith et al., 1994); anti-acetylated-α-tubulin mouse monoclonal antibody (1/150, Sigma); anti-glu-α-tubulin mouse monoclonal antibody (clone 1D5; 1/100, Synaptic Systems), mouse nestin antibody (1/400, BD Pharmigen), rabbit anti-ZO1 antibody (1/200, Zymed Laboratories), rabbit anti-GFAP antibody (1/300, DakoCytomation) and rabbit anti-Glu-tubulin (1/100, Abcys). Immunostaining was revealed with donkey anti-rabbit biotinylated antibody (1/400, Jackson, Interchim) and Cy3-conjuguated streptavidin (1/400, Interchim) or anti mouse-Alexa-Fluor-488-conjugated antibodies (1/400, Molecular Probes). The slides were mounted in the presence of DAPI or TOPRO3 in Vectashield (Vectors Laboratory) mounting medium. For CD24 staining, rat anti-CD24 antibody (1/200, BD Pharmingen) was used and no Triton X-100 was included during incubations. After incubation with the secondary antibodies (goat biotinylated anti-rat antibody, Vector Laboratories and Cy3-conjuguated streptavidin, Interchim), cells were post-fixed in 4% paraformaldehyde for 10 minutes at room temperature and processed for other primary antibodies with 0.1% Triton X-100. Slides were visualized under an inverted Zeiss Axiovert fluorescent microscope equipped with 20× Plan-neofluar (0.5 numerical aperture) or 40× Plan-neofluar (0.75 numerical aperture) objectives. Controls in which individual primary antibodies were omitted resulted in no detectable staining. Images were acquired with a CCD camera (HQ2, Roper-Scientific) and Metaview software (Roper Scientific). Image brightness and contrast were adjusted by using ImageJ (NIH image) and separate panels were assembled with Photoshop 9.02 software. Capture times and adjustments were identical for images mounted together. Quantification of immunofluorescence was performed on confocal stacks acquired with a Zeiss LSM510 Meta confocal microscope and processed with MetaMorph software (Molecular Devices).

Cilia counting and density

For quantification of cilia, ten different fields from wild-type or *Rfx3*$^{-/-}$ cell cultures were photographed. Cilia were counted and classified into six categories: monocilia, 3 cilia/cell, 5-10 cilia/cell, 10-15 cilia/cell, 20-30 cilia/cell and 40 cilia/cell and above. Scatter-plot analysis was performed to report the number of monociliated cells (first category) or multiciliated cells (five other categories combined) relative to the total number of nuclei for each field for seven wild-type samples and seven *Rfx3*$^{-/-}$ samples. Correlation was calculated using a linear regression model and statistical significance of the variations between the linear regression slopes were evaluated.

CBF measurements

Beating cilia were observed using an oil-immersion microscope (Leica DM-RXA) at a magnification of 100× for room-temperature measurements and an inverted microscope (Olympus IX-50) at a magnification of 40× for measurements in a temperature-controlled chamber at 37°C. Beating cilia were recorded with a digital high-speed video camera (PCO.1200hs, PCO.imaging, Germany) at a rate of 500 frames per second. The video sequences were extracted and recorded by ImageJ followed by reslicing to visualize and measure the time period (in seconds) of individual beating cilia. For the calculation of CBF and the statistical comparison between *Rfx3*$^{+/+}$ and *Rfx3*$^{-/-}$ ependymal cilia, six to nine different fields were recorded and analyzed for each sample. For two litters (nos 5 and 6), CBFs were measured and analyzed in the same way on three different days (4 days between each measurement, first measure at day 16) for all the *Rfx3*$^{-/-}$ (n=4) and *Rfx3*$^{+/+}$ (n=7) littermates. The last measurement was performed at 37°C. A total of 407 fields were video recorded and analyzed (one to three cells/field and one to three cilia/cell). Statistical analysis was performed using ANOVA and a linear mixed effect model. P-values of <0.05 were considered statistically significant. Movies from acquired stacks were made with ImageJ software (Sorensen compression).

Ciliary length

Immunofluorescence images of cilia stained with detyrosinated or acetylated α-tubulin were acquired in 20-30 consecutive z-stack slices (depending on the length of cilia) using a Leica confocal microscope (TCS SP5) with a 63× objective. The z-stack images were flattened using Leica confocal software (LCS Lite, v2.61). Cilia length was measured directly using a graphical pencil. 3D depictions of cilia were reconstructed using IMARIS software (Bitplane). Statistical significance of the differences in ciliary length between wild-type and *Rfx3*$^{-/-}$ samples was evaluated using a two-sample Student's t-test.

Electron microscopy

Cells were fixed in 2.0% glutaraldehyde in 0.1 M sodium cacodylate, pH 7.35, for 45 minutes at room temperature. After extensive washing in sodium cacodylate 0.2 M, pH 7.35, cells were post-fixed in 1% OsO_4 for 30 minutes, stained with uranyl acetate 1% for 30 minutes and dehydrated using a graded ethanol series. Cells were embedded in epoxy resin. Ultrafine sections were cut with a Leica ultramicrotome. Sectioned materials were contrasted in Leica ultrastainer in lead citrate. Sections were observed with a Philips CM120 microscope.

Real-time RT-PCR

Total RNA was extracted using the Nucleospin RNA kit (Macherey Nagel). cDNA was synthesized using 0.5 μg of total RNA, 200 ng of random primers (Promega) and 200 units of RevertAid H Minus M-MuLV Reverse Transcriptase (Fermentas) according to the manufacturer's protocol in a final volume of 50 μl. Real-time PCR was performed on 5 μl of cDNA diluted 1/10 using the SYBR Green fluorescent mix (Roche) in a LightCycler LC480 (Roche). Primer sequences are available upon request. According to melting-point analysis, only one PCR product was amplified. RNA extracted from wild-type samples was used to generate a standard quantification curve for each gene, allowing the calculation of relative amounts of transcripts in the samples. For time-course expression analysis, reactions were performed for five or six independent cultures. The expression of each gene was normalized using the housekeeping gene *Tbp* (TATA binding protein) (Vandesompele et al., 2002), which was selected because it is expressed in a range similar to that of ciliary genes. The results were expressed relative to day 0 (set at 1). Statistical significance of the differences in gene expression between day 0 and each of the other days was evaluated with a two-tailed paired Student's *t*-test. For mRNA expression in wild-type and *Rfx3*$^{-/-}$ backgrounds, reactions were performed with ten *Rfx3*$^{+/+}$ and five *Rfx3*$^{-/-}$ samples, except for *Bbs4* and *Foxj1*, for which 14 wild-type and 11 *Rfx3*$^{-/-}$ samples were analyzed. Statistical analysis was performed with Kruskal-Wallis non-parametric analysis of variance.

Chromatin immunoprecipitation

Brains from 40 newborn pups (OF1 strain) were dissected and processed as above for cell cultures. After 12 days of serum deprivation, cells were fixed and processed for ChIP experiments as described previously (Masternak and Reith, 2002) using antibodies specific for RFX3 (Reith et al., 1994). Results were quantified by real-time PCR using the primers listed in supplementary material Table S1. PCR was performed using the iCycler iQ Real-Time PCR Detection System (Bio-Rad) and a SYBR-Green-based kit for quantitative PCR (iQ Supermix Bio-Rad). All results are presented as the mean ± s.e.m. of three independent ChIP experiments and three independent amplifications. X-box motifs were identified with Genepalette software (Rebeiz and Posakony, 2004) using the degenerate consensus defined for RFX proteins in mammals RYYNYYN$_{0\text{-}3}$RRNRAC (Emery et al., 1996b). Each X-box motif was checked for sequence conservation between mammalian species using the UCSC genome browser. Only one conserved X-box motif was generally found in the 2-kb region upstream of the transcription start site. ChIP primers were designed at positions flanking the conserved X-box sequences. For *Dnahc5*, several pairs of primers were tested in a region covering 2-kb upstream of the transcription start site.

Online supplementary information

Supplementary material Table S1 lists the primers used for the ChIP experiments. Supplementary material Movie 1 shows OF1 cultures after 20 days of serum deprivation imaged at ten frames per second by DIC videomicroscopy and played at real speed. Supplementary material Movie 2 shows *Rfx3*$^{+/+}$ beating cilia imaged at 500 frames per second by DIC videomicroscopy and played at a tenfold reduced speed. Supplementary material Movie 3 shows *Rfx3*$^{-/-}$ beating cilia observed by DIC videomicroscopy and played at a tenfold reduced speed. Supplementary material Fig. S1 summarizes cell-culture characteristics before and after serum deprivation. Supplementary material Fig. S2 shows basal-body and cilia ultrastructure of wild-type and Rfx3$^{-/-}$ samples.

This work was supported by grants from the ANR Jeune-Chercheur, the ANR Maladies Rare (ANR-05-MRAR-022-01) and the Région Rhône-Alpes (Programme Emergence, Programme Cible). Work in the laboratory of W.R. was supported by the Swiss National Science Foundation and the National Centre of Competence in Research NCCR-NEURO. A.A.-L. was supported by fellowships from the Association de Langue Française pour l'Etude du Diabète et des Maladies Métaboliques (ALFEDIAM), the Jules Thorn Foundation and the EFSD/Lilly program. We thank Guillaume Tanniou for helpful assistance with mouse care and genotyping and Julien Falk for help with brain dissection of the subventricular zone. We are grateful to Hadrien Charvat, Mohamad Arzi and Sylvain Mousset for statistical analysis, and Denis Ressnikoff and Béatrice Burdin for technical assistance in confocal microscopy. Lastly, we thank Elisabeth Cortier, Jean-Luc Duteyrat, Annie Rivoire and Christelle Boule for excellent technical assistance in electron microscopy. Experiments were performed with the help of the electron microscopy facility (CTmu) and of the Centre Commun de Quantimétrie (CCQ) of the University of Lyon.

References

Aftab, S., Semenec, L., Chu, J. S. and Chen, N. (2008). Identification and characterization of novel human tissue-specific RFX transcription factors. *BMC Evol. Biol.* **8**, 226.

Ait-Lounis, A., Baas, D., Barras, E., Benadiba, C., Charollais, A., Nlend Nlend, R., Liegeois, D., Meda, P., Durand, B. and Reith, W. (2007). Novel function of the ciliogenic transcription factor RFX3 in development of the endocrine pancreas. *Diabetes* **56**, 950-959.

Andersen, J. S., Wilkinson, C. J., Mayor, T., Mortensen, P., Nigg, E. A. and Mann, M. (2003). Proteomic characterization of the human centrosome by protein correlation profiling. *Nature* **426**, 570-574.

Ansley, S. J., Badano, J. L., Blacque, O. E., Hill, J., Hoskins, B. E., Leitch, C. C., Kim, J. C., Ross, A. J., Eichers, E. R., Teslovich, T. M. et al. (2003). Basal body dysfunction is a likely cause of pleiotropic Bardet-Biedl syndrome. *Nature* **425**, 628-633.

Avidor-Reiss, T., Maer, A. M., Koundakjian, E., Polyanovsky, A., Keil, T., Subramaniam, S. and Zuker, C. S. (2004). Decoding cilia function: defining specialized genes required for compartmentalized cilia biogenesis. *Cell* **117**, 527-539.

Baas, D., Meiniel, A., Benadiba, C., Bonnafe, E., Meiniel, O., Reith, W. and Durand, B. (2006). A deficiency in RFX3 causes hydrocephalus associated with abnormal differentiation of ependymal cells. *Eur. J. Neurosci.* **24**, 1020-1030.

Bartoloni, L., Blouin, J. L., Pan, Y., Gehrig, C., Maiti, A. K., Scamuffa, N., Rossier, C., Jorissen, M., Armengot, M., Meeks, M. et al. (2002). Mutations in the DNAH11 (axonemal heavy chain dynein type 11) gene cause one form of situs inversus totalis and most likely primary ciliary dyskinesia. *Proc. Natl. Acad. Sci. USA* **99**, 10282-10286.

Beckers, A., Alten, L., Viebahn, C., Andre, P. and Gossler, A. (2007). The mouse homeobox gene Noto regulates node morphogenesis, notochordal ciliogenesis, and left right patterning. *Proc. Natl. Acad. Sci. USA* **104**, 15765-15770.

Bisgrove, B. W. and Yost, H. J. (2006). The roles of cilia in developmental disorders and disease. *Development* **133**, 4131-4143.

Blackshear, P. J., Graves, J. P., Stumpo, D. J., Cobos, I., Rubenstein, J. L. and Zeldin, D. C. (2003). Graded phenotypic response to partial and complete deficiency of a brain-specific transcript variant of the winged helix transcription factor RFX4. *Development* **130**, 4539-4552.

Blacque, O. E., Perens, E. A., Boroevich, K. A., Inglis, P. N., Li, C., Warner, A., Khattra, J., Holt, R. A., Ou, G., Mah, A. K. et al. (2005). Functional genomics of the cilium, a sensory organelle. *Curr. Biol.* **15**, 935-941.

Blatt, E. N., Yan, X. H., Wuerffel, M. K., Hamilos, D. L. and Brody, S. L. (1999). Forkhead transcription factor HFH-4 expression is temporally related to ciliogenesis. *Am. J. Respir. Cell Mol. Biol.* **21**, 168-176.

Bonnafe, E., Touka, M., AitLounis, A., Baas, D., Barras, E., Ucla, C., Moreau, A., Flamant, F., Dubruille, R., Couble, P. et al. (2004). The transcription factor RFX3 directs nodal cilium development and left-right asymmetry specification. *Mol. Cell. Biol.* **24**, 4417-4427.

Bonneau, D., Raymond, F., Kremer, C., Klossek, J. M., Kaplan, J. and Patte, F. (1993). Usher syndrome type I associated with bronchiectasis and immotile nasal cilia in two brothers. *J. Med. Genet.* **30**, 253-254.

Broadhead, R., Dawe, H. R., Farr, H., Griffiths, S., Hart, S. R., Portman, N., Shaw, M. K., Ginger, M. L., Gaskell, S. J., McKean, P. G. et al. (2006). Flagellar motility is required for the viability of the bloodstream trypanosome. *Nature* **440**, 224-227.

Brody, S. L., Yan, X. H., Wuerffel, M. K., Song, S. K. and Shapiro, S. D. (2000). Ciliogenesis and left-right axis defects in forkhead factor HFH-4-null mice. *Am. J. Respir. Cell Mol. Biol.* **23**, 45-51.

Calaora, V., Chazal, G., Nielsen, P. J., Rougon, G. and Moreau, H. (1996). mCD24 expression in the developing mouse brain and in zones of secondary neurogenesis in the adult. *Neuroscience* **73**, 581-594.

Carson, J. L., Reed, W., Lucier, T., Brighton, L., Gambling, T. M., Huang, C. H. and Collier, A. M. (2002). Axonemal dynein expression in human fetal tracheal epithelium. *Am. J. Physiol. Lung Cell Mol. Physiol.* **282**, L421-L430.

Chen, J., Knowles, H. J., Hebert, J. L. and Hackett, B. P. (1998). Mutation of the mouse hepatocyte nuclear factor/forkhead homologue 4 gene results in an absence of cilia and random left-right asymmetry. *J. Clin. Invest.* **102**, 1077-1082.

Chen, N., Mah, A., Blacque, O. E., Chu, J., Phgora, K., Bakhoum, M. W., Hunt Newbury, C. R., Khattra, J., Chan, S., Go, A. et al. (2006). Identification of ciliary and ciliopathy genes in Caenorhabditis elegans through comparative genomics. *Genome Biol.* **7**, R126.

Driscoll, J. A., Bhalla, S., Liapis, H., Ibricevic, A. and Brody, S. L. (2008). Autosomal dominant polycystic kidney disease is associated with an increased prevalence of radiographic bronchiectasis. *Chest* **133**, 1181-1188.

Dubruille, R., Laurencon, A., Vandaele, C., Shishido, E., Coulon-Bublex, M., Swoboda, P., Couble, P., Kernan, M. and Durand, B. (2002). Drosophila regulatory factor X is necessary for ciliated sensory neuron differentiation. *Development* **129**, 5487-5498.

Efimenko, E., Bubb, K., Mak, H. Y., Holzman, T., Leroux, M. R., Ruvkun, G., Thomas, J. H. and Swoboda, P. (2005). Analysis of xbx genes in C. elegans. *Development* **132**, 1923-1934.

Efimenko, E., Blacque, O. E., Ou, G., Haycraft, C. J., Yoder, B. K., Scholey, J. M., Leroux, M. R. and Swoboda, P. (2006). Caenorhabditis elegans DYF-2, an orthologue of human WDR19, is a component of the intraflagellar transport machinery in sensory cilia. *Mol. Biol. Cell* **17**, 4801-4811.

Eggenschwiler, J. T. and Anderson, K. V. (2007). Cilia and developmental signaling. *Annu. Rev. Cell Dev. Biol.* **23**, 345-373.

Emery, P., Durand, B., Mach, B. and Reith, W. (1996a). RFX proteins, a novel family of DNA binding proteins conserved in the eukaryotic kingdom. *Nucleic Acids Res.* **24**, 803-807.

Emery, P., Strubin, M., Hofmann, K., Bucher, P., Mach, B. and Reith, W. (1996b). A consensus motif in the RFX DNA binding domain and binding domain mutants with altered specificity. *Mol. Cell. Biol.* **16**, 4486-4494.

Fliegauf, M., Olbrich, H., Horvath, J., Wildhaber, J. H., Zariwala, M. A., Kennedy, M., Knowles, M. R. and Omran, H. (2005). Mislocalization of DNAH5 and DNAH9 in Respiratory Cells from Patients with Primary Ciliary Dyskinesia. *Am. J. Respir. Crit. Care Med.* **171**, 1343-1349.

Fliegauf, M., Benzing, T. and Omran, H. (2007). When cilia go bad: cilia defects and ciliopathies. *Nat. Rev. Mol. Cell Biol.* **8**, 880-893.

Gajiwala, K. S., Chen, H., Cornille, F., Roques, B. P., Reith, W., Mach, B. and Burley, S. K. (2000). Structure of the winged -helix protein hRFX1 reveals a new mode of DNA binding. *Nature* **403**, 916-921.

Gherman, A., Davis, E. E. and Katsanis, N. (2006). The ciliary proteome database: an integrated community resource for the genetic and functional dissection of cilia. *Nat. Genet.* **38**, 961-962.

Gomperts, B. N., Gong-Cooper, X. and Hackett, B. P. (2004). Foxj1 regulates basal body anchoring to the cytoskeleton of ciliated pulmonary epithelial cells. *J. Cell Sci.* **117**, 1329-1337.

Gresh, L., Fischer, E., Reimann, A., Tanguy, M., Garbay, S., Shao, X., Hiesberger, T., Fiette, L., Igarashi, P., Yaniv, M. et al. (2004). A transcriptional network in polycystic kidney disease. *EMBO J.* **23**, 1657-1668.

Haycraft, C. J., Swoboda, P., Taulman, P. D., Thomas, J. H. and Yoder, B. K. (2001). The C. elegans homolog of the murine cystic kidney disease gene Tg737 functions in a ciliogenic pathway and is disrupted in osm-5 mutant worms. *Development* **128**, 1493-1505.

Haycraft, C. J., Schafer, J. C., Zhang, Q., Taulman, P. D. and Yoder, B. K. (2003). Identification of CHE-13, a novel intraflagellar transport protein required for cilia formation. *Exp. Cell Res.* **284**, 249-261.

Hayes, J. M., Kim, S. K., Abitua, P. B., Park, T. J., Herrington, E. R., Kitayama, A., Grow, M. W., Ueno, N. and Wallingford, J. B. (2007). Identification of novel ciliogenesis factors using a new in vivo model for mucociliary epithelial development. *Dev. Biol.* **312**, 115-130.

Huang, T., You, Y., Spoor, M. S., Richer, E. J., Kudva, V. V., Paige, R. C., Seiler, M. P., Liebler, J. M., Zabner, J., Plopper, C. G. et al. (2003). Foxj1 is required for apical localization of ezrin in airway epithelial cells. *J. Cell Sci.* **116**, 4935-4945.

Ibanez-Tallon, I., Gorokhova, S. and Heintz, N. (2002). Loss of function of axonemal dynein Mdnah5 causes primary ciliary dyskinesia and hydrocephalus. *Hum. Mol. Genet.* **11**, 715-721.

Inglis, P. N., Boroevich, K. A. and Leroux, M. R. (2006). Piecing together a ciliome. *Trends Genet.* **22**, 491-500.

Keller, L. C., Romijn, E. P., Zamora, I., Yates, J. R., 3rd and Marshall, W. F. (2005). Proteomic analysis of isolated chlamydomonas centrioles reveals orthologs of ciliary-disease genes. *Curr. Biol.* **15**, 1090-1098.

Koudritsky, M. and Domany, E. (2008). Positional distribution of human transcription factor binding sites. *Nucleic Acids Res.* **36**, 6795-6805.

Laurencon, A., Dubruille, R., Efimenko, E., Grenier, G., Bissett, R., Cortier, E., Rolland, V., Swoboda, P. and Durand, B. (2007). Identification of novel regulatory factor X (RFX) target genes by comparative genomics in Drosophila species. *Genome Biol.* **8**, R195.

Li, J. B., Gerdes, J. M., Haycraft, C. J., Fan, Y., Teslovich, T. M., May-Simera, H., Li, H., Blacque, O. E., Li, L., Leitch, C. C. et al. (2004). Comparative genomics identifies a flagellar and basal body proteome that includes the BBS5 human disease gene. *Cell* **117**, 541-552.

Liu, Y., Pathak, N., Kramer-Zucker, A. and Drummond, I. A. (2007). Notch signaling controls the differentiation of transporting epithelia and multiciliated cells in the zebrafish pronephros. *Development* **134**, 1111-1122.

Lonergan, K. M., Chari, R., Deleeuw, R. J., Shadeo, A., Chi, B., Tsao, M. S., Jones, S., Marra, M., Ling, V., Ng, R. et al. (2006). Identification of novel lung genes in bronchial epithelium by serial analysis of gene expression. *Am. J. Respir. Cell Mol. Biol.* **35**, 651-661.

Marshall, W. F. (2008). The cell biological basis of ciliary disease. *J. Cell Biol.* **180**, 17-21.

Masternak, K. and Reith, W. (2002). Promoter-specific functions of CIITA and the MHC class II enhanceosome in transcriptional activation. *EMBO J.* **21**, 1379-1388.

McClintock, T. S., Glasser, C. E., Bose, S. C. and Bergman, D. A. (2008). Tissue expression patterns identify mouse cilia genes. *Physiol. Genomics* **32**, 198-206.

Moore, A., Escudier, E., Roger, G., Tamalet, A., Pelosse, B., Marlin, S., Clement, A., Geremek, M., Delaisi, B., Bridoux, A. M. et al. (2006). RPGR is mutated in patients with a complex X linked phenotype combining primary ciliary dyskinesia and retinitis pigmentosa. *J. Med. Genet.* **43**, 326-333.

Olbrich, H., Haffner, K., Kispert, A., Volkel, A., Volz, A., Sasmaz, G., Reinhardt, R., Hennig, S., Lehrach, H., Konietzko, N. et al. (2002). Mutations in DNAH5 cause primary ciliary dyskinesia and randomization of left-right asymmetry. *Nat. Genet.* **30**, 143-144.

Osman, E. M., Abboud, O. I., Sulaiman, S. M., Musa, A. R., Beleil, O. M. and Sharfi, A. A. (1991). End-stage renal failure in Kartagener's syndrome. *Nephrol. Dial. Transplant.* **6**, 747.

Ostrowski, L. E., Blackburn, K., Radde, K. M., Moyer, M. B., Schlatzer, D. M., Moseley, A. and Boucher, R. C. (2002). A proteomic analysis of human cilia: identification of novel components. *Mol. Cell Proteomics* **1**, 451-465.

Pazour, G. J., Agrin, N., Leszyk, J. and Witman, G. B. (2005). Proteomic analysis of a eukaryotic cilium. *J. Cell Biol.* **170**, 103-113.

Rebeiz, M. and Posakony, J. W. (2004). GenePalette: a universal software tool for genome sequence visualization and analysis. *Dev. Biol.* **271**, 431-438.

Reith, W., Ucla, C., Barras, E., Gaud, A., Durand, B., Herrero-Sanchez, C., Kobr, M. and Mach, B. (1994). RFX1, a transactivator of hepatitis B virus enhancer I, belongs to a novel family of homodimeric and heterodimeric DNA-binding proteins. *Mol. Cell. Biol.* **14**, 1230-1244.

Ross, A. J., Dailey, L. A., Brighton, L. E. and Devlin, R. B. (2007). Transcriptional profiling of mucociliary differentiation in human airway epithelial cells. *Am. J. Respir. Cell Mol. Biol.* **37**, 169-185.

Schafer, J. A., Haycraft, C. J., Thomas, J. H., Yoder, B. K. and Swoboda, P. (2003). xbx-1 encodes a dynein light intermediate chain (DLIC) required for retrograde intraflagellar transport and cilia assembly in *C. elegans. Mol. Biol. Cell* **14**, 2057-2070.

Schwabe, G. C., Hoffmann, K., Loges, N. T., Birker, D., Rossier, C., de Santi, M. M., Olbrich, H., Fliegauf, M., Failly, M., Liebers, U. et al. (2008). Primary ciliary dyskinesia associated with normal axoneme ultrastructure is caused by DNAH11 mutations. *Hum. Mutat.* **29**, 289-298.

Shah, A. S., Farmen, S. L., Moninger, T. O., Businga, T. R., Andrews, M. P., Bugge, K., Searby, C. C., Nishimura, D., Brogden, K. A., Kline, J. N. et al. (2008). Loss of Bardet-Biedl syndrome proteins alters the morphology and function of motile cilia in airway epithelia. *Proc. Natl. Acad. Sci. USA* **105**, 3380-3385.

Singla, V. and Reiter, J. F. (2006). The primary cilium as the cell's antenna: signaling at a sensory organelle. *Science* **313**, 629-633.

Spassky, N., Merkle, F. T., Flames, N., Tramontin, A. D., Garcia-Verdugo, J. M. and Alvarez-Buylla, A. (2005). Adult ependymal cells are postmitotic and are derived from radial glial cells during embryogenesis. *J. Neurosci.* **25**, 10-18.

Stolc, V., Samanta, M. P., Tongprasit, W. and Marshall, W. F. (2005). Genome-wide transcriptional analysis of flagellar regeneration in Chlamydomonas reinhardtii identifies orthologs of ciliary disease genes. *Proc. Natl. Acad. Sci. USA* **102**, 3703-3707.

Stubbs, J. L., Oishi, I., Izpisua Belmonte, J. C. and Kintner, C. (2008). The forkhead protein Foxj1 specifies node-like cilia in Xenopus and zebrafish embryos. *Nat. Genet.* **40**, 1454-1460.

Supp, D. M., Witte, D. P., Potter, S. S. and Brueckner, M. (1997). Mutation of an axonemal dynein affects left-right asymmetri in inersus viscerum mice. *Nature* **389**, 963-966.

Swoboda, P., Adler, H. T. and Thomas, J. H. (2000). The RFX-type transcription factor DAF-19 regulates sensory neuron cilium formation in C. elegans. *Mol. Cell* **5**, 411-421.

Tabach, Y., Brosh, R., Buganim, Y., Reiner, A., Zuk, O., Yitzhaky, A., Koudritsky, M., Rotter, V. and Domany, E. (2007). Wide-scale analysis of human functional transcription factor binding reveals a strong bias towards the transcription start site. *PLoS ONE* **2**, e807.

Tichelaar, J. W., Wert, S. E., Costa, R. H., Kimura, S. and Whitsett, J. A. (1999). HNF-3/forkhead homologue-4 (HFH-4) is expressed in ciliated epithelial cells in the developing mouse lung. *J. Histochem. Cytochem.* **47**, 823-832.

Toskala, E., Smiley-Jewell, S. M., Wong, V. J., King, D. and Plopper, C. G. (2005). Temporal and spatial distribution of ciliogenesis in the tracheobronchial airways of mice. *Am. J. Physiol. Lung Cell Mol. Physiol.* **289**, L454-L459.

Vandesompele, J., De Preter, K., Pattyn, F., Poppe, B., Van Roy, N., De Paepe, A. and Speleman, F. (2002). Accurate normalization of real-time quantitative RT-PCR data by geometric averaging of multiple internal control genes. *Genome Biol.* **3**, RESEARCH0034.

Whitsett, J. A. and Tichelaar, J. W. (1999). Forkhead transcription factor HFH-4 and respiratory epithelial cell differentiation. *Am. J. Respir. Cell Mol. Biol.* **21**, 153-154.

You, Y., Huang, T., Richer, E. J., Schmidt, J. E., Zabner, J., Borok, Z. and Brody, S. L. (2004). Role of f-box factor foxj1 in differentiation of ciliated airway epithelial cells. *Am. J. Physiol. Lung Cell Mol. Physiol.* **286**, L650-L657.

Yu, X., Ng, C. P., Habacher, H. and Roy, S. (2008). Foxj1 transcription factors are master regulators of the motile ciliogenic program. *Nat. Genet.* **40**, 1445-1453.

Zhang, D., Zeldin, D. C. and Blackshear, P. J. (2007). Regulatory factor X4 variant **3**, a transcription factor involved in brain development and disease. *J. Neurosci. Res.* **85**, 3515-3522.

Journal of Cell Science